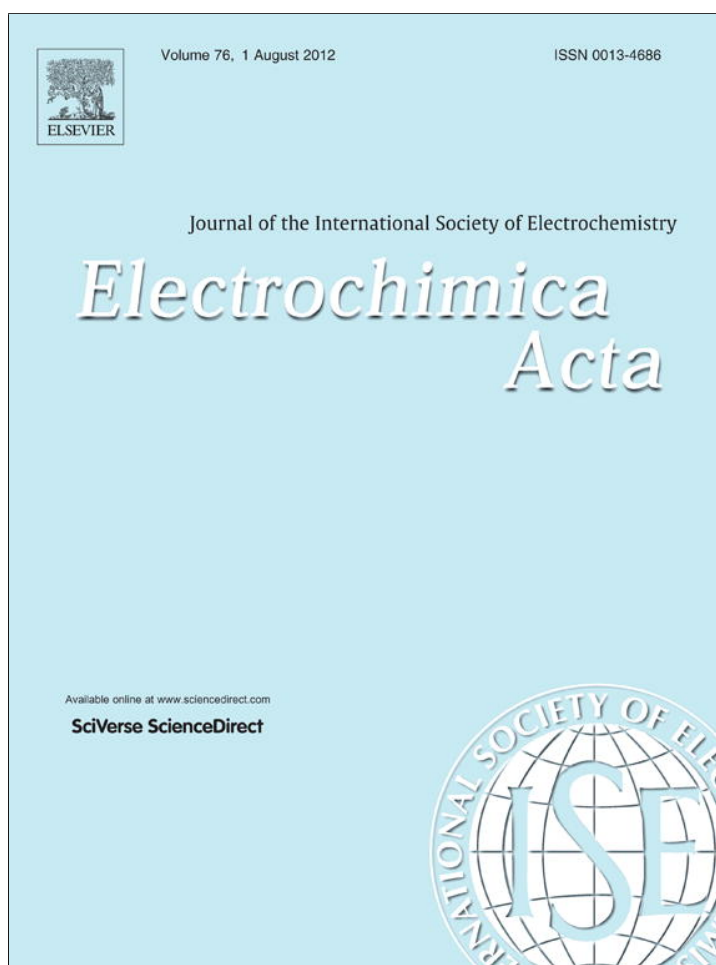


Provided for non-commercial research and education use.
Not for reproduction, distribution or commercial use.



This article appeared in a journal published by Elsevier. The attached copy is furnished to the author for internal non-commercial research and education use, including for instruction at the authors institution and sharing with colleagues.

Other uses, including reproduction and distribution, or selling or licensing copies, or posting to personal, institutional or third party websites are prohibited.

In most cases authors are permitted to post their version of the article (e.g. in Word or Tex form) to their personal website or institutional repository. Authors requiring further information regarding Elsevier's archiving and manuscript policies are encouraged to visit:

<http://www.elsevier.com/copyright>



Ni nanoparticles decorated titania nanotube arrays as efficient nonenzymatic glucose sensor

Shujuan Yu^a, Xiao Peng^{b,*}, Guozhong Cao^c, Ming Zhou^a, Lei Qiao^a, Jianyu Yao^a, Huichao He^a

^a College of Chemical Engineering, Chongqing University, Chongqing 400044, China

^b College of Physics, Chongqing University, Chongqing 400044, China

^c Department of Materials Science & Engineering, University of Washington, Seattle, WA 98195, USA

ARTICLE INFO

Article history:

Received 23 December 2011

Received in revised form 19 May 2012

Accepted 25 May 2012

Available online 2 June 2012

Keywords:

Glucose sensor

Ni nanoparticles

TiO₂ nanotube arrays

Nonenzymatic

Electrocatalysis

ABSTRACT

A novel nonenzymatic glucose sensor was developed based on the Ni nanoparticles-loaded TiO₂ nanotube arrays (Ni-NPs/TiO₂NTs). The Ni-NPs/TiO₂NTs nanocomposites were prepared first by anodization of Ti foil, followed by pulsed electrodeposition method (PED) and characterized by SEM, XRD and XPS respectively. The results showed that spherical Ni nanoparticles were well dispersed and embedded in the TiO₂NTs. The electrochemical measurements presented that the activated Ni-NPs with a diameter of 40 nm displayed high electrocatalytic activity for the oxidation of glucose and a good sensitivity of 700.2 $\mu\text{A mM}^{-1} \text{cm}^{-2}$ at applied potential 0.6V, with detection limit of 2 μM ($S/N=3$), and good linear range (from 0.004 to 4.8 mM). Such high sensitivity was attributed to the large surface area of the highly dispersed nanoparticles for electrocatalytic reaction and the fast electron transfer in the TiO₂NTs electrode. The good analytical performance, low cost and simple preparation method make this novel electrode material promising for the development of effective glucose nonenzymatic glucose sensor.

© 2012 Elsevier Ltd. All rights reserved.

1. Introduction

The unique and fascinating properties of nanostructured materials have attracted tremendous attention among scientists to explore the full potential to use them in sensor applications. Glucose biosensors, as the most popular biosensors, have been extensively investigated due to their important applications in clinical diagnosis, pharmaceutical analysis and food industry [1,2]. Based on the electrochemical method, enzyme-involved glucose sensors have been widely studied because of its high selectivity and sensitivity [3–5]. The activity of enzyme, however, is easily influenced by temperature, humidity and chemical environment (e.g., pH), which will cause the instability of the biosensor [6]. To address this problem, nonenzymatic glucose sensors consisting of metal nanoparticles/carbon nanotubes (CNTs) aroused interest in many studies. By unique properties of metal nanoparticles such as enhancing mass transport, high catalysis and increasing surface areas, various metal nanoparticles modified electrode such as Pt [7–9], Au [10,11], Ag [12], Cu [13,14], Ni [15,16], Pd [17], alloy [18–20] exhibited high electrocatalytic activity for the oxidation of glucose. It was also well-known that the performance of the sensor heavily relies on the matrix CNTs properties, such as its excellent electron transfer rate and electrocatalytic activities [21,22].

Recently, TiO₂ nanotube arrays (TiO₂NTs) fabricated by anodization of titanium substrate have been studied directly for biosensor applications [23,24] or used as the supporting electrode for loading [25,26] and dispersing metal nanoparticles for sensor applications [27,28]. As an active matrix, TiO₂NTs possess high specific surface area and well-aligned nanostructures with good adhesion to the substrate. In addition, each channel of a nanotube on the TiO₂NTs electrode serves as an independent nano-sized reaction chamber, metal nanoparticles adsorbed onto the surface both sides of nanotubes retain high specific surface area. Most importantly, according to our previous studies, the average apparent heterogeneous electron transfer rate constant (k) was $2.18 \times 10^{-3} \text{ cm/s}$ for TiO₂NTs modified by surface defects. This result can match with the electron transfer rate constant of carbon nanotubes ($7.53 \times 10^{-4} \text{ cm s}^{-1}$) [29,30]. Furthermore, TiO₂NTs have superior bio-affinity. Therefore they are very promising supporting matrix for loading metal nanoparticles for the development of nonenzymatic glucose sensors.

Ni-based nonenzymatic sensors were extensively investigated for electrocatalytic oxidation of glucose [15,31]. The oxidation processes are catalyzed by the Ni-based sensors through the formation of a high-valent, oxyhydroxide species (NiOOH) in alkaline medium. Most Ni-based sensors were prepared by modifying electrodes with Ni nanoparticles, such as electrospinning Ni nanoparticles on carbon nanofibers or dispersing Ni nanoparticles in disordered graphite-like carbon [15,32]. Such Ni nanoparticles-based electrode demonstrated drastic improvements in terms of

* Corresponding author. Tel.: +86 23 65678362; fax: +86 23 65102031.

E-mail address: xiaopeng@cqu.edu.cn (X. Peng).

glucose detection sensitivity, compared to the Ni plate. But the agglomeration of Ni nanoparticles remained a big challenge [15,32]. In addition, the stability and catalytic activity of the nanoparticles depended strongly on the size, morphology, and distribution of the nanoparticles. It remains another great challenge to minimize the agglomeration of Ni nanoparticles, so as to improve their catalytic activities for the development of Ni nanoparticles-based glucose sensor.

This paper reports for the first time the fabrication of highly dispersed Ni nanoparticles in TiO₂NTs (Ni-NPs/TiO₂NTs) as a transducer for a nonenzymatic glucose sensor. The fabrication process mainly includes two steps: The first step is the anodic growth of TiO₂NTs from a Ti foil and doping surface oxygen vacancies by annealing method, while the second step is the pulse electrodeposition (PED) of well dispersed Ni nanoparticles into TiO₂NTs. In comparison with conventional electrodeposition with a constant DC current, PED favors the initial nucleation with much increased number of nuclei per unit surface area, resulting in many tiny sized nanoparticles deposited [33,34]. It was demonstrated that TiO₂NTs doped with oxygen vacancies could be an inexpensive alternative to carbon nanotubes as support for the metal nanoparticles catalysts. The Ni-NPs/TiO₂NTs electrode displayed high sensitivity, fast response and a wide linear range for glucose detection. The size effect of Ni nanoparticles of the sensor was also studied.

2. Experimental

2.1. Reagents and apparatus

Titanium foil (purity: 99.9% Ti, 0.5 mm thick) were purchased from Goodfellow Cambridge Ltd. Glucose, ascorbic acid (AA) and uric acid (UA) were purchased from Sigma and used without further purification. Hydrofluoric acid (HF, 40%), boracic acid (H₃BO₃), nickel sulfate hexahydrate (NiSO₄·6H₂O) and nickel chloride hexahydrate (NiCl₂·6H₂O) were purchased from ChuanDong Ltd. All Chemicals were of analytical grade and without further purifications. All the solutions were prepared with deionized water.

2.2. Preparation of Ni-NPs/TiO₂NTs

Well-aligned titania nanotube arrays were prepared by the anodization method [35]. The growth conditions used in this work are similar to those reported in our earlier publications [31]. The as-anodized TiO₂ nanotubes were annealed in a tube furnace under a flow of dry nitrogen atmosphere with a heating rate of 4 °C min⁻¹ and a dwelling time of 3 h at 400 °C. Ni nanoparticles were electrodeposited into the annealed TiO₂NTs electrode by PED [36]. Deposition experiments were performed in a three-electrode system (TiO₂NTs as a working electrode, nickel plate as a counter electrode and Ag/AgCl electrode as a reference electrode). The electrolyte consisted of 300 g/L NiSO₄·6H₂O, 45 g/L NiCl₂·6H₂O, 37 g/L H₃BO₃, pH = 4.4 and the temperature was kept at 38 °C. Pulse electrodeposition parameters include negative current (−160 mA cm⁻², 8 ms) and positive current (160 mA cm⁻², 2 ms), current off-time (1000 ms), and deposition time (20 min, 25 min and 30 min). The electrodes deposited for 20 min, 25 min and 30 min are denoted as sample B, sample C and sample D respectively. After deposition, the Ni-NPs/TiO₂NTs were first sealed with epoxy resin leaving an open area of 1 cm² as the prepared electrode.

The as-prepared Ni-NPs/TiO₂NTs were characterized by scanning electron microscopy (SEM, Nova 400 Nano-SEM, 20 kV), X-ray diffraction (XRD, Shimadzu ZD-3AX, Cu K α radiation) and XPS (ESCALAB 250, Thermo Fisher Scientific) respectively. Electrodeposition experiments were carried out on Autolab PGSTAT30 workstation.

2.3. Electrochemical measurements

Electrochemical measurements were performed using CHI660C (Shanghai, China) with a three electrode system consisting of the prepared electrode as working electrode, a platinum wire as counter electrode and an Ag/AgCl (sat. KCl) as reference electrode. Firstly, before glucose detection, Ni-NPs/TiO₂NTs electrodes (1 cm²) were activated by using successively cyclic sweeps between 0.2 and 0.6 V at 50 mV s⁻¹ in 0.1 M NaOH solution, until a stable CV profile was obtained. The activated Ni-NPs/TiO₂NTs electrodes were evaluated as a glucose sensor in 0.1 M NaOH solution at room temperature. Different concentrations of glucose were prepared in 0.1 M NaOH solution before use. Amperometric curves were obtained when desired concentration of glucose were successively added into the cell containing 100 mL of 0.1 M NaOH solution under stirring.

3. Results and discussion

3.1. Characterization of the Ni-NPs/TiO₂NTs

Fig. 1 shows the FESEM images of TiO₂NTs before and after incorporated by Ni nanoparticles, the deposition times of sample B, C and D were 20, 25 and 30 min respectively. The average pore diameters of TiO₂NTs are about 100 nm and the thickness of the wall is about 15 nm (Fig. 1A). Oxygen vacancies on TiO₂NTs surface created by annealing treatment can bind molecules or act as preferential adsorption sites for metallic nanoparticles. Thus, Ni nanoparticles were loaded effectively by PED method in the tubes. With the increase of deposition time, more and more nickel nanoparticles loaded on TiO₂NTs can be observed (Fig. 1B, C and D). At the same time, the average size of the nanoparticles become larger and larger increased from about 20 to 85 nm, which is attributed to be inclined to reduce the surface energy of the nanoparticles for the further nucleation and growth of Ni. As can be seen from inset of Fig. 1B, highly dispersed Ni nanoparticles are evenly distributed on the side wall of TiO₂NTs. In addition, because of the unique structure of TiO₂NTs, Ni nanoparticles embedded in TiO₂NTs tubes have higher surface area than those loaded on a flat electrode. Thus Ni nanoparticles modified TiO₂NTs have more active sites for detecting glucose.

Fig. 2A shows the XRD pattern of TiO₂NTs (i) and Ni-NPs/TiO₂NTs (ii) respectively. The peak with 2 θ of 25.3° is assigned to an anatase crystal structure of TiO₂NTs (Fig. 2A(i)). After electrodeposition, the diffraction peaks at 44.5° and 51.8° correspond to Ni (1 1 1) and (2 0 0), respectively (Fig. 2A(ii)). XPS measurement was carried out to further confirm the composition of Ni nanoparticles. As demonstrated in Fig. 2B, the Ni 2p_{3/2} XPS peaks (and the associated satellites) located at binding energies of 852.7 and 855.6 eV (satellite at 861.5 eV with respect to the main signal) correspond to metallic Ni and Ni(OH)₂, respectively, which is in agreement with the results of a previous report on nanocrystalline Ni coatings [37], indicating that the presence of metallic Ni and Ni(OH)₂ on the surface of as-prepared sample. This is because with the increase of the deposition time, hydrogen evolution reaction on the surface of electrode led to the increase of OH⁻ concentration in electrolyte solution. Simultaneously, Ni absorbed water molecules reacted with OH⁻ and produced nickel hydroxide passive films on nanoparticle surface [37]. But due to the small quantity, the Ni(OH)₂ could not be detected by the XRD measurement. So the nanoparticles were composed by a large amount of nickel and a small quantity of Ni(OH)₂.

Incorporation of nanoparticles into TiO₂NTs by chemical bath method and electrochemical deposition method has been reported [38,39]. However, deposition of highly dispersed metal

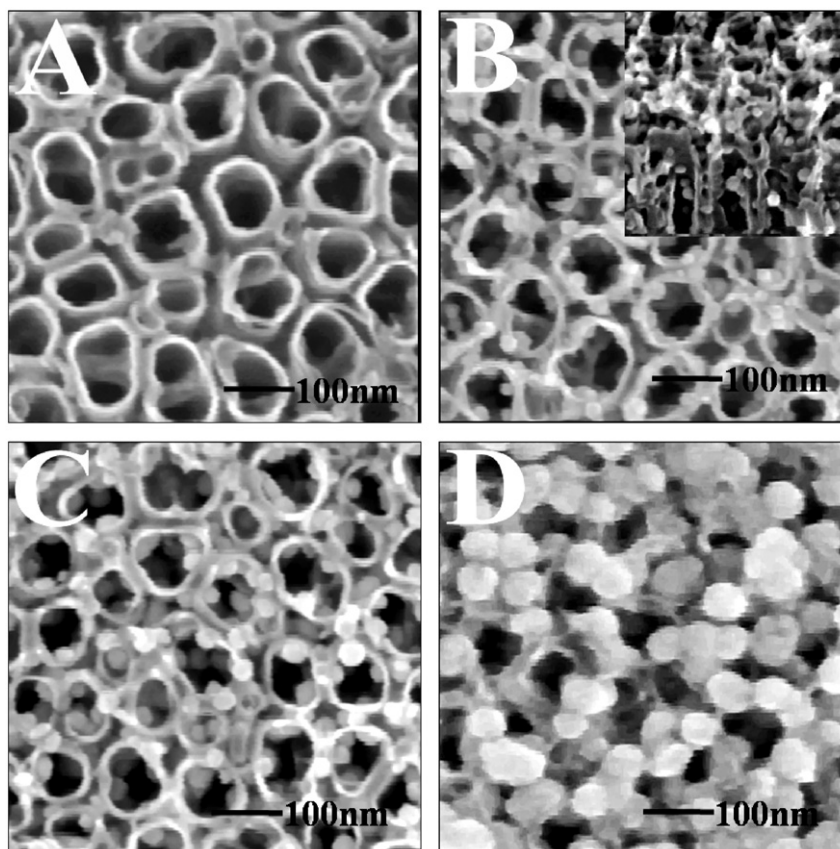


Fig. 1. FESEM images of TiO₂NTs (A) and Ni-NPs/TiO₂NTs deposited for different time: (B) 20 min; (C) 25 min; (D) 30 min. Inset: the cross-sectional FESEM image of sample C.

nanoparticles into the nanochannels of TiO₂NTs is difficult to achieve because of the greater inertness and small size of these channels. Here a simple and effective way was introduced. The first stage was associated with the reduction of TiO₂NTs surface by annealing method to create oxygen vacancies and increase metal nucleation. For example, Besenbacher et al. [40] reported that oxygen vacancies allowed for the stabilization of gold monomers and gold trimers. This means that metal clusters readily nucleate homogeneously on reduced TiO₂NTs and form highly dispersed nanocrystals. The second procedure involved the application of PED technique. In electrochemical deposition process, the factors that influence the formation of new crystals include (i) high adatoms population, (ii) high overpotential and (iii) low surface diffusion rate. By employing high peak current density (I_p) in PED

method, the crystallization overpotential was increased, which in turn improved the nucleation rate resulting in finer crystals.

3.2. Electrocatalytic oxidation of glucose at activated Ni-NPs/TiO₂NTs

It was reported that the nickel-based catalysts exhibited high electrocatalytic activity toward the oxidation of organic molecules in alkaline medium, this effect involved electron transfer mediation by Ni(OH)₂/NiOOH redox couple in the oxide film at the electrode surface. Moreover, most oxidizable organic compounds were found to oxidize at the same potential and this potential coincided exactly with that at which the surface of the nickel electrode becomes oxidized. Thus, to form more Ni²⁺/Ni³⁺ redox couples on the

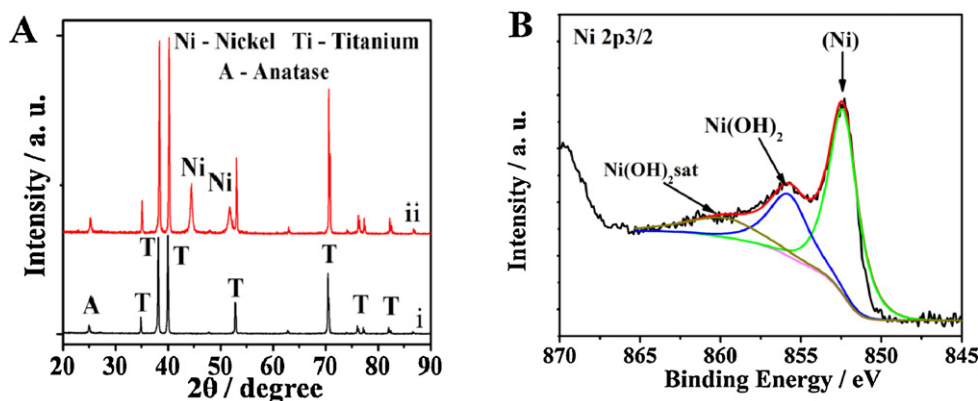


Fig. 2. (A) XRD patterns of TiO₂NTs (i) and Ni-NPs/TiO₂NTs (ii). (B) XPS spectra of Ni-NPs/TiO₂NTs at the peak Ni 2p_{3/2}.

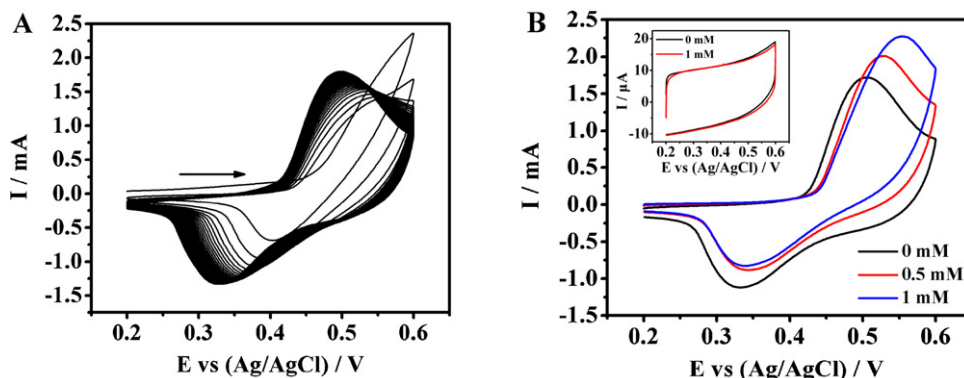


Fig. 3. (A) CVs of as-prepared Ni-NPs/TiO₂NTs in 0.1 M NaOH solution at the scan rate of 50 mV s⁻¹ for 50 cycles. (B) CVs of activated Ni-NPs/TiO₂NTs in the absence and presence of 0.5 mM, 1 mM glucose respectively in 0.1 M NaOH solution. Inset: CVs of TiO₂NTs in 0.1 M NaOH solution in the absence and presence of 1 mM glucose. Scan rate: 50 mV s⁻¹.

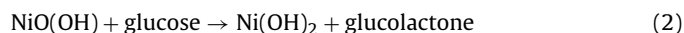
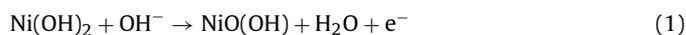
Ni-NPs, the as-prepared Ni-NPs/TiO₂NTs were first activated in 0.1 M NaOH.

Fig. 3A presents the consecutive cyclic voltammetric of the Ni-NPs/TiO₂NTs (sample C) in 0.1 M NaOH solution at a scan rate of 50 mV s⁻¹. The first cyclic voltammetric corresponded with the oxidation of Ni to Ni(OH)₂ in alkaline solution, then Ni(OH)₂ was progressively oxidized to NiOOH with the increase of scanning cycles. So, a pair of well-defined redox peaks with cathodic peaks at 326 mV and the anodic peaks at 499 mV was observed in the CV results, corresponding to the Ni²⁺/Ni³⁺ redox couples. The anodic and cathodic peaks current increased as the cycle number increased and then a current plateau and stable voltammetric response was obtained after 50 scanning cycles, implying that the oxidation of Ni-NPs/TiO₂NTs reached a steady state. The obtained stable anodic current was about 1.686 mA, the larger current may be attributed to a good electrochemical performance of anatase TiO₂NTs annealed in N₂ and high loading amount of Ni nanoparticles inside the tubes.

Fig. 3B shows CVs response of the activated Ni-NPs/TiO₂NTs (sample C) in 0.1 M NaOH solution containing different concentrations of glucose. One pair of well-defined redox peaks was observed at 336 mV and 499 mV in the absence of glucose (black line), which could be attributed to Ni²⁺/Ni³⁺ redox group forming in the alkaline medium. When 0.5 mM glucose was addition to the NaOH solution, notable enhancement of the anodic current could be observed, and the voltammetric response increased with a rising concentration of glucose. Therefore, the activated Ni-NPs/TiO₂NTs exhibited electrocatalytic performance for oxidation of glucose as expected. In order to understand if the bare TiO₂NT was involved in the electrocatalytic process, CV experiment was also performed at the bare TiO₂NTs in the absence and presence of 1 mM glucose (Fig. 3B, inset). The result showed that there was a mild current response after the addition of glucose and no obvious redox peaks were observed for the bare TiO₂NTs. The weak current difference might

be due to the glucose degradation at the bare TiO₂NTs. While the anodic current response for the activated Ni-NPs/TiO₂NTs in presence of 1 mM glucose was about 559 μA so that the activated nanoparticles played a significant role in electrocatalytic detection of glucose.

The sensing mechanism of the electrode is schematically shown in Fig. 4. In alkaline solution, Ni³⁺ formed on the nanoparticles surface rapidly oxidized glucose to gluconolactone. At the same time, the consumption of Ni³⁺ species and the production of Ni²⁺ species resulted in the increase of oxidation peak current and the decrease of reduction peak current. Here the Ni³⁺ species might act as an electron-transfer mediator. The response mechanism of the activated Ni-NPs/TiO₂NTs to electrochemical oxidation of glucose can be simply expressed as [41]:



3.3. Amperometric responses of glucose at activated Ni-NPs/TiO₂NTs

The amperometric responses of Ti foil, bare TiO₂NTs and activated Ni-NPs/TiO₂NTs for a successive addition of 0.5 mM glucose at 50 s intervals in 0.1 M NaOH at optimal potential of 0.6 V are shown in Fig. 5A. No obvious response current of Ti foil and bare TiO₂NTs can be observed. As expected, the activated Ni-NPs/TiO₂NTs produced significantly response signals. This obvious response concurred with high electrocatalysis of activated Ni nanoparticles.

Fig. 5B shows the amperometric responses for the successive additions of 10 μM glucose in 0.1 M NaOH solution at 0.6 V of the activated Ni-NPs/TiO₂NTs deposited under different times respectively. It was observed that the electrodes responded quickly to the

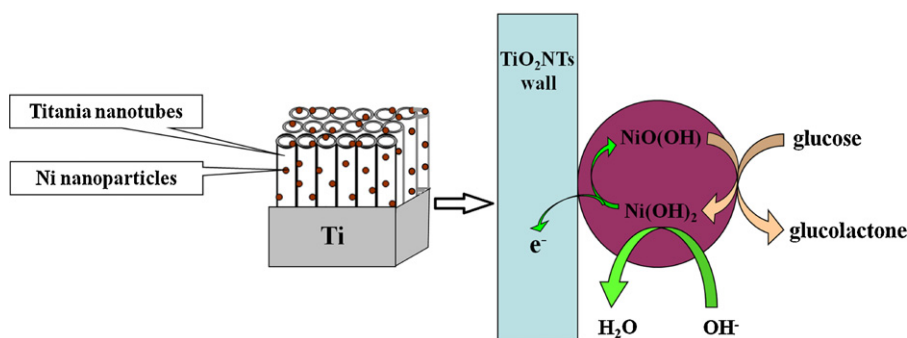


Fig. 4. Schematic representation of activated Ni-NPs/TiO₂NTs and its glucose sensing mechanism.

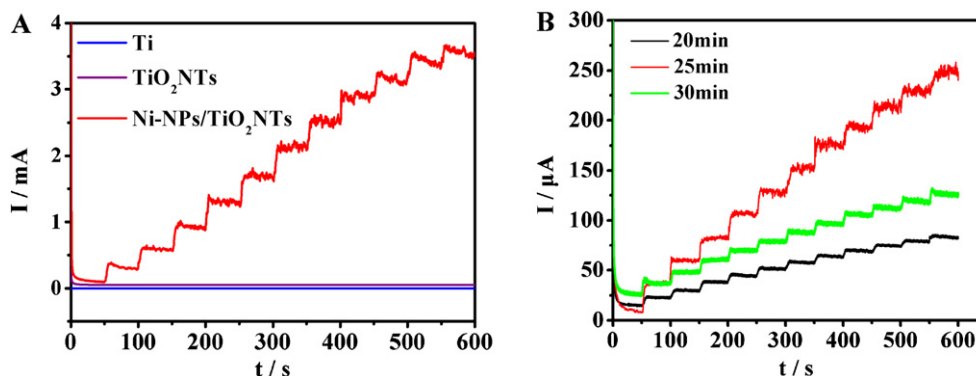


Fig. 5. Amperometric responses of Ti, bare TiO₂NTs and activated Ni-NPs/TiO₂NTs for successive additions of 0.5 mM glucose in 0.1 M NaOH solution at 0.6 V, respectively. (B) Amperometric responses for successive additions of 10 μM glucose in 0.1 M NaOH solution at 0.6 V of activated Ni-NPs/TiO₂NTs deposited for different times: 20 min, 25 min, and 30 min respectively.

change of glucose concentration and reached a steady-state signal within 5 s. Moreover, the size effect of Ni nanoparticles for the oxidation of glucose was studied. The current response of sample C to 10 μM glucose was about 25 μA, which was significantly higher than those of the other two electrodes. It should be noted that the Ni nanoparticles of sample D had the greatest size (~85 nm) and deposition quantity, while the sample B had the smallest size (~20 nm) and quantity. Thus, it could be deduced both the deposition quantity and nanoparticles size obviously influenced the response of the electrode, more nickel quantity was not always helpful for the response. It was reported that the catalytic performance of nanomaterial was related on surface effects due to boundary conditions, which depended on the surface-to-volume ratio, the shape and size [42]. For example, the catalytic activity of Au nanoparticles increased with the decrease of the particle size in the certain range [43]. It was shown from the Fig. 1 that the Ni nanoparticles size became larger and larger with the increase of deposition time, which led to the decrease of specific surface area of Ni nanoparticles and then reduced catalysis. Although sample B had the smallest particle size, its deposition quantity was very low due to the short deposition time, thus its catalytic activity was not as high as sample C.

According to the above results, we chose the activated Ni-NPs/TiO₂NTs prepared at deposition time of 25 min (sample C) to obtain the sensing performance. The influence of the applied potential on the response of the sensor was investigated. Current-time curves were recorded at different applied potential in successive addition 0.5 mM glucose (not shown). The results showed that the best sensing respond was observed at the applied potential of 0.6 V.

Fig. 6A shows the amperometric responses of the activated Ni-NPs/TiO₂NTs (sample C) upon successive addition of various concentrations of glucose at the applied potential of 0.6 V. The response time was less than 5 s, indicating a good catalytic property of the electrode. The corresponding calibration curve (Fig. 6A, right inset) was linear from 0.004 to 4.8 mM with a sensitivity of 700.2 μA mM⁻¹ cm⁻² and a detection limit of 2 μM (S/N = 3).

The sensing performance of the sensor was compared with the previously reported glucose sensors based on the utilization of Ni nanoparticles modified electrodes as shown in Table 1. It was concluded that our activated Ni-NPs/TiO₂NTs has a higher sensitivity and a wider linear range. This result also verified that TiO₂NTs could be used as a good substrate material for sensors. Moreover, the sensitivity of the Ni-NPs/TiO₂NTs was greatly higher than that of Ni layers modified TiO₂NTs (200 μA mM⁻¹ cm⁻²) [44]. The higher sensitivity was attributed to a good conductivity and unique surface structure of TiO₂NTs and high electrocatalytic activity of dispersed Ni nanoparticles with high surface areas.

3.4. Anti-interferences, reproducibility and stability of activated Ni-NPs/TiO₂NTs

The presence of electroactive compounds in real blood, such as AA and UA, interferences the determination of glucose. Therefore, we examined the electrochemical response of UA and AA at activated Ni-NPs/TiO₂NTs. The experiment was carried out by adding 1.0 mM glucose in 0.1 M NaOH followed by 0.01 mM AA and 0.01 mM UA. As shown in Fig. 6B, the electroactive species did not cause interference significantly for the determination of glucose.

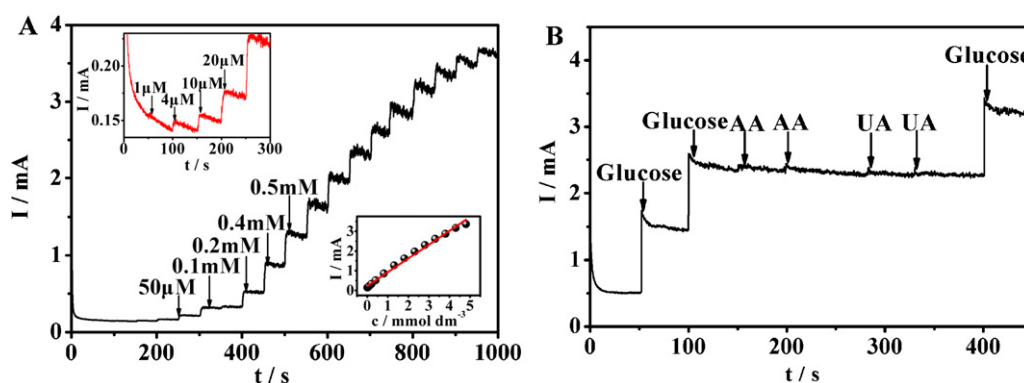


Fig. 6. (A) Typical amperometric response of activated Ni-NPs/TiO₂NTs (sample C) towards various concentrations of glucose at 0.6 V in 0.1 M NaOH solution; left inset: the amplified response curve, right inset: the linear calibration curve. (B) Interference test of the activated Ni-NPs/TiO₂NTs to the successive addition of 1 mM glucose, 0.01 mM AA, and 0.01 mM UA.

Table 1Comparison of the performance parameters of the activated Ni-NPs/TiO₂NTs (sample C) and Ni nanoparticles modified electrodes.

Electrode materials	Sensitivity	Linear range (mmol l ⁻¹)	Detection limit (μmol l ⁻¹)	Ref.
Ni nanoparticle-loaded carbon nanofiber paste electrode	0.003 mA mmol ⁻¹ cm ⁻²	0.002–2.5	1	[15]
Ni nanoparticles embedded in a graphite-like carbon film electrode	Not given	0.00005–0.5	0.02	[32]
Ni–Pd nanoparticles 3D ordered silicon microchannel plate	0.081 mA mM ⁻¹	Not given	5	[45]
Ni nanoparticles modified TiO ₂ NTs electrode	0.700 mA mM ⁻¹ cm ⁻²	0.004–4.8	2	Present work

These results implied that the activated Ni-NPs/TiO₂NTs has a good anti-interference ability.

Six successive measurements of glucose on one Ni-NPs/TiO₂NTs yielded an R.S.D. of 4.1%, indicating that the sensor was reproducible. The stability was studied by successively scanning in 0.1 M NaOH solution after storing 20 days. The stable oxidation current decreased to 80.3% of its initial response.

4. Conclusions

An enzyme-free glucose sensor was fabricated by pulsed electrochemical deposition of Ni nanoparticles into highly ordered TiO₂ nanotubes. Due to unique structure of the nanotubes and high surface areas of the deposited nanoparticles, Ni-NPs with a diameter of 40 nm exhibited high electrocatalytic activity for the glucose electro-oxidation. The activated Ni-NPs/TiO₂NT demonstrated a detection limit of 2 μM, high sensitivity of 700.2 μA mM⁻¹ cm⁻² and a wide linear range of 4 μM to 4.8 mM. The excellent sensing performance, low cost and simple fabrication procedure may potentially pave the way for large scale production of inexpensive, effective and highly sensitive glucose sensors.

Acknowledgement

This work was supported by the Fundamental Research Funds for the Central Universities (Project No. CDJZR10100021).

References

- [1] J. Wang, *Chemical Reviews* 108 (2008) 814.
- [2] L.A. Terry, S.F. White, L.J. Tigwell, *Journal of Agricultural and Food Chemistry* 53 (2005) 1309.
- [3] J. Lu, L.T. Drzal, R.M. Worden, I. Lee, *Chemistry of Materials* 19 (2007) 6240.
- [4] M. Zhou, L. Shang, B.L. Li, L.J. Huang, S.J. Dong, *Biosensors and Bioelectronics* 24 (2008) 442.
- [5] W.J. Li, R. Yuan, Y.Q. Chai, H.A. Zhong, Y. Wang, *Electrochimica Acta* 56 (2011) 4203.
- [6] R. Wilson, A.P.F. Turner, *Biosensors and Bioelectronics* 7 (1992) 165.
- [7] D. Rathod, C. Dickinson, D. Egan, E. Dempsey, *Sensors and Actuators B* 143 (2010) 547.
- [8] L.Q. Rong, C. Yang, Q.Y. Qian, X.H. Xia, *Talanta* 72 (2007) 819.
- [9] G. Wei, F.G. Xu, Z. Li, K.D. Jandt, *Journal of Physical Chemistry C* 115 (2011) 11453.
- [10] H. Zhu, X.Q. Lu, M.X. Li, Y.H. Shao, Z.W. Zhu, *Talanta* 79 (2009) 1446.
- [11] L. Zhou, T. Gan, D.Y. Zheng, J.J. Yan, C.G. Hu, S.S. Hu, *Journal of Experimental Nanoscience* 7 (2012) 263.
- [12] A. Baciú, A. Pop, A. Remes, F. Manea, G. Burtica, *Advanced Science Engineering and Medicine* 3 (2011) 13.
- [13] L.M. Lu, X.B. Zhang, G.L. Shen, R.Q. Yu, *Analytica Chimica Acta* 715 (2012) 99.
- [14] H.X. Wu, W.M. Cao, Y. Li, G. Liu, Y. Wen, H.F. Yang, S.P. Yang, *Electrochimica Acta* 55 (2010) 3734.
- [15] Y. Liu, H. Teng, H.Q. Hou, T.Y. You, *Biosensors and Bioelectronics* 24 (2009) 3329.
- [16] J.H. Zhu, J. Jiang, J.P. Liu, R.M. Ding, Y.Y. Li, H. Ding, Y.M. Feng, G.M. Wei, X.T. Huang, *RSC Advances* 1 (2011) 1020.
- [17] H.F. Cui, J.S. Ye, W.D. Zhang, C.M. Li, J.H.T. Luong, F.S. Sheu, *Analytica Chimica Acta* 594 (2007) 175.
- [18] D.Y. Liu, Q.M. Luo, F.Q. Zhou, *Electrochimica Acta* 56 (2011) 5855.
- [19] J. Ryu, K. Kim, H.S. Kim, H.T. Hahn, D. Lashmore, *Biosensors and Bioelectronics* 26 (2010) 602.
- [20] A.H. Liu, H.R. Geng, C.X. Xu, H.J. Qiu, *Analytica Chimica Acta* 703 (2011) 172.
- [21] J. Lu, I. Do, L.T. Drzal, R.M. Worden, I. Lee, *ACS Nano* 2 (2008) 1825.
- [22] L.N. Cella, W. Chen, N.V. Myung, A. Mulchandani, *Journal of the American Chemical Society* 132 (2010) 5024.
- [23] P. Xiao, B.B. Garcia, Q. Guo, D.W. Liu, G.Z. Cao, *Electrochemistry Communications* 9 (2007) 2441.
- [24] A.K.M. Kafi, G.S. Wu, P. Benvenuto, A.C. Chen, *Journal of Electroanalytical Chemistry* 662 (2011) 64.
- [25] J.M. Macak, F. Schmidt-Stein, P. Schmuki, *Electrochemistry Communications* 9 (2007) 1783.
- [26] A. Honciuc, M. Laurin, S. Albu, M. Amende, M. Sobota, R. Lynch, P. Schmuki, J. Libuda, *Journal of Physical Chemistry C* 114 (2010) 20146.
- [27] X.Y. Pang, D.M. He, S.L. Luo, Q.Y. Cai, *Sensors and Actuators B* 137 (2009) 134.
- [28] S. Mahshid, C.C. Li, S.S. Mahshid, M. Askari, A. Dolati, L.X. Yang, S.L. Luo, Q.Y. Cai, *Analyst* 136 (2011) 2322.
- [29] Y.H. Zhang, P. Xiao, X.Y. Zhou, D.W. Liu, B.B. Garcia, G.Z. Cao, *Journal of Materials Chemistry* 19 (2009) 948.
- [30] P. Xiao, H.L. Fang, G.Z. Cao, Y.H. Zhang, X.X. Zhang, *Thin Solid Films* 518 (2010) 7152.
- [31] A. Safavi, N. Maleki, E. Farjami, *Biosensors and Bioelectronics* 24 (2009) 1655.
- [32] T.Y. You, O. Niwa, Z.L. Chen, K. Hayashi, M. Tomita, S. Hirono, *Analytical Chemistry* 75 (2003) 5191.
- [33] M.S. Chandrasekar, M. Pushpavanam, *Electrochimica Acta* 53 (2008) 3313.
- [34] K. Nielsch, F. Müller, A.P. Li, U. Gösele, *Advanced Materials* 12 (2000) 582.
- [35] D. Gong, C.A. Grimes, O.K. Varghese, W.C. Hu, R.S. Singh, Z. Chen, E.C. Dickey, *Journal of Materials Research* 16 (2001) 3331.
- [36] Y.H. Zhang, Y.N. Yang, P. Xiao, X.N. Zhang, L. Lu, L. Li, *Materials Letters* 63 (2009) 2429.
- [37] L.P. Wang, J.Y. Zhang, Y. Gao, Q.J. Xue, L.T. Hu, T. Xu, *Scripta Materialia* 55 (2006) 657.
- [38] S.G. Chen, M. Paulose, C. Ruan, G.K. Mor, O.K. Varghese, D. Kouzoudis, C.A. Grimes, *Journal of Photochemistry and Photobiology A: Chemistry* 177 (2006) 177.
- [39] I. Paramasivam, J.M. Macak, P. Schmuki, *Electrochemistry Communications* 10 (2008) 71.
- [40] D. Matthey, J.G. Wang, S. Wendt, J. Matthesen, R. Schaub, E. Lægsgaard, B. Hammer, F. Besenbacher, *Science* 315 (2007) 1692.
- [41] L.M. Lu, L. Zhang, F.L. Qu, H.X. Lu, X.B. Zhang, Z.S. Wu, S.Y. Huan, Q.A. Wang, G.L. Shen, R.Q. Yu, *Biosensors and Bioelectronics* 25 (2009) 218.
- [42] G.A. Somorjai, Y.G. Borodko, *Catalysis Letters* 76 (2001) 1.
- [43] M. Comotti, C. Della Pina, R. Matarrese, M. Rossi, *Angewandte Chemie International Edition* 43 (2004) 5812.
- [44] C.X. Wang, L.W. Yin, L.Y. Zhang, R. Gao, *Journal of Physical Chemistry C* 114 (2010) 4408.
- [45] F.J. Miao, B.R. Tao, L. Sun, T. Liu, J.C. You, L.W. Wang, P.K. Chu, *Sensors and Actuators B* 141 (2009) 338.